ELSEVIER

Journal of Molecular Catalysis A: Chemical 139 (1999) 285–303

JOURNAL OF MOLECULAR CATALYSIS A: CHEMICAL

IR study of CO adsorption on Cu–Rh/SiO_2 catalysts, coked by reaction with methane

James A. Anderson, Colin H. Rochester *, Zhuojian Wang

Chemistry Department, Dundee University, Dundee DD1 4HN, UK

Received 16 January 1998; accepted 5 June 1998

Abstract

Infrared spectra are reported of CO adsorbed on silica-supported Rh, Cu, and Cu–Rh catalysts before and after coking by heat treatment in methane at 673 K, and after subsequent exposure to hydrogen at 293, 373 or 473 K. The surface of Cu–Rh particles was enriched with copper, but all surfaces contained alloy phases. Addition of copper to rhodium blocked sites for the formation of $Rh(CO)_2$, decreased the proportion of sites which linearly adsorbed CO, but favoured bridge-bonded CO on Rh sites. Cu sites in Cu/SiO_2 were not poisoned by methane treatment, but Cu sites and all types of Rh site in Cu–Rh/SiO_2 underwent poisoning in the sequence Cu–CO > Rh–CO > $Rh_2CO \approx Rh_2(CO)_3$. CO band shifts caused by coking of rhodium sites are attributed to a decrease in dipolar coupling. Dipole coupling changes were more significant when the Rh surface was modified by Cu than by coking. Coke deposits, at least in the presence of CO, aggregated into patches on exposed Rh surfaces. Similar effects of coking occurred for linear CO on copper sites. Rh/SiO_2 gave a high yield of methane, but only a low yield of ethane on coke hydrogenation. Copper largely poisoned the catalytic activity, which it is tentatively proposed primarily involved sites on rhodium which adsorb CO in a bridging configuration.

Keywords: Cu–Rh/SiO_2; Methane activation; CO adsorption

1. Introduction

It has been shown that the conversion of methane to higher hydrocarbons over heterogeneous catalysts may be achieved by a two-stage process involving methane decomposition at high temperature to carbonaceous residue followed by the reaction of the residue with hydrogen at lower temperature [1–3]. Several types of carbonaceous residue have been identified and have been found to differ in their reactivity towards hydrogen [2–4]. Supported rhodium catalysts promote methane activation [2,5–7], although the nature of the carbonaceous species obtained may be influenced by the oxide support [5–7]. The stepwise conversion of methane to ethane over copper is unsatisfactory [2]. However, mixing copper and rhodium in Cu–Rh/SiO_2 catalysts has been shown to enhance the formation of ethane from methane [8]. Different studies of supported Cu–Rh catalysts have apparently established that enrichment with either copper [9,10] or rhodium [11] may occur at the particle surfaces.

* Corresponding author.

1381-1169/99/$ - see front matter
PII: S1381-1169(98)00206-4

Infrared spectra of adsorbed carbon monoxide can give valuable information about surface sites in mixed metal catalysts [12], spectra for $Cu–Rh/SiO_2$ exhibiting bands due to CO adsorbed on both the rhodium and copper components of the catalyst [11]. Here, CO is used to probe the mixed metal surfaces of $Cu–Rh/SiO_2$ before and after high-temperature treatment in methane, and after subsequent treatment in hydrogen, in order to assess which sites are influenced by carbonaceous residue.

2. Experimental

Catalysts were prepared by initially evaporating to dryness a dispersion of silica (Degussa Aerosil, 200 $m^2\ g^{-1}$) in an aqueous solution of copper (II) acetate and/or rhodium (III) nitrate. The resulting powder was dried (383 K, 16 h) and then calcined in a flow of dry CO_2-free air for 1 h at 673 K before storage as catalyst precursor. Loosely powdered precursor was used in the flow reactor or in the hydrogen chemisorption cell. Infrared spectroscopy involved the use of self-supporting discs of precursor pressed at 30 MN m^{-2} pressure. In all experiments, reduction involved heat treatment (673 K, 2 h) in a flow (100 $cm^3\ min^{-1}$ at 1 atm) of hydrogen admitted via a Deoxo unit and 4 Å molecular sieve. Metal contents of reduced catalysts are given in Table 1.

After reduction catalyst discs in infrared experiments involving CO adsorption were evacuated for 10 min at 673 K before being cooled to room temperature for spectroscopic examination using a Perkin Elmer 1720 FTIR spectrometer operating at 4 cm^{-1} resolution. Coking of reduced catalysts involved initial evacuation at 673 K for 20 min followed by exposure to 2.00 kN m^{-2} methane for 10 min at 673 K, evacuation for 10 min at 673 K and cooling to ca. 293 K before admission of CO. In separate experiments, catalysts after coking were evacuated at 673 K for 10 min, cooled and exposed to hydrogen (1.33 kN m^{-2}) at 293, 373 or 473 K for 15 min, evacuated at the temperature of hydrogen treatment for 10 min and cooled to ca. 293 K before admission of CO.

Hydrogen chemisorption at ca. 293 K was used to assess numbers of surface rhodium atoms in the Rh and Cu–Rh catalysts [10,13]. The pre-treatment conditions for obtaining reduced catalysts and catalysts coked by reaction with methane at 673 K were identical to those adopted in the infrared experiments.

The reaction of hydrogen with the carbonaceous deposits generated by catalyst treatment with methane were investigated in the range ca. 325–475 K by GC analysis of the effluent gases using a Perkin Elmer 8410 gas chromatograph with a flame ionisation detector. Preparation of coked catalysts in the reactor involved contact at 673 K with a flow of methane at 1 atm for 18 min, followed by the removal of methane with a flow of nitrogen gas (10 $cm^3\ min^{-1}$, 1 atm) at 773 K. After coking, the catalyst was cooled to ca. 325 K in the nitrogen flow, the nitrogen was then replaced by hydrogen (30 $cm^3\ min^{-1}$, 1 atm) and the temperature was gradually ramped up to ca. 475 K, analyses being carried out at ca. 25-K intervals.

Table 1
Metal contents of catalysts after reduction in hydrogen

Catalyst designation	Cu/wt.%	Rh/wt.%	mol Cu + Rh per g silica	Cu/Rh mol ratio
Cu/SiO_2	1.00	0	1.59×10^{-4}	1:0
$Cu–Rh(A)/SiO_2$	1.50	3.40	5.96×10^{-4}	1:1.4
$Cu–Rh(B)/SiO_2$	1.11	5.04	7.07×10^{-4}	1:2.8
$Cu–Rh(C)/SiO_2$	0.73	6.63	8.19×10^{-4}	1:5.6
$Rh(A)/SiO_2$	0	2.78	2.78×10^{-4}	0:1
$Rh(B)/SiO_2$	0	5.00	5.11×10^{-4}	0:1

3. Results

3.1. CO adsorption on Rh/SiO_2

Spectra of CO adsorbed on $Rh(B)/SiO_2$ are shown in Fig. 1. Dominant maxima at 2071 cm^{-1} and 1888 cm^{-1}, shifting to 1898 cm^{-1} with increasing CO pressure, may be ascribed to linear and bridged CO, respectively, adsorbed on the rhodium surface [14–16]. Weaker bands at 2095 and 2031 cm^{-1} were due to rhodium gem-dicarbonyl species [14,17]. A shoulder at 1965 cm^{-1} resembles a band at 1949 cm^{-1}, previously ascribed for CO on Rh/SiO_2 [15] to bridging CO in a $Rh_2(CO)_3$ structure [18]. Evacuation for 20 min caused an 18% reduction in the intensity of the band due to linear CO, and a band shift to 2058 cm^{-1}. The strong band due to bridged species was unchanged in intensity, but gradually shifted to 1870 cm^{-1} during evacuation. The gem-dicarbonyl species was also resistant to desorption at 293 K, although the shoulder at 2095 cm^{-1} became a maximum at 2097 cm^{-1} and the maximum at 2033 cm^{-1} became a shoulder because of the shift of the band due to linearly adsorbed CO towards lower wave numbers.

Heat treatment of $Rh(B)/SiO_2$ in methane caused a decrease in the intensities of infrared bands resulting from the adsorption of CO (Fig. 2). In the presence of 3.6 kN m^{-2}, CO the band due to linearly adsorbed CO appeared at 2060 cm^{-1} for the methane-treated surface and was 70% weaker in intensity than that for the untreated catalyst. The band shift from 2071 to 2060 cm^{-1} induced by methane treatment may be ascribed at least in part to a decrease in dipole coupling between adjacent CO molecules [18] caused by poisoning of some of the CO adsorption sites by the products of decomposition of methane. However, Solymosi and Lancz [18] suggested that a further contributing factor to the effect of surface carbon on adsorbed CO is electron donation from carbon to rhodium, which enhances back donation into the antibonding $\pi*$ orbital of CO, thus, weakening the CO bond [18]. The band due to bridged CO was 38% weaker for the methane-treated surface than for the untreated catalyst, and for the former, the band was shifted to 1855 cm^{-1} at high

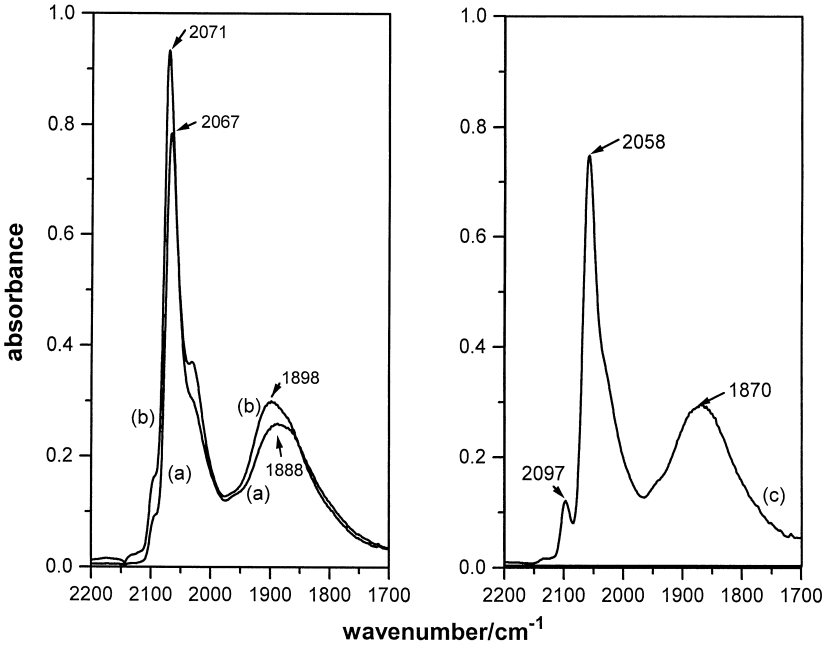

Fig. 1. Spectra of $Rh(B)/SiO_2$ after the addition of CO at (a) < 0.1 and (b) 3.6 kN m^{-2}, and (c) subsequent evacuation (293 K, 20 min).

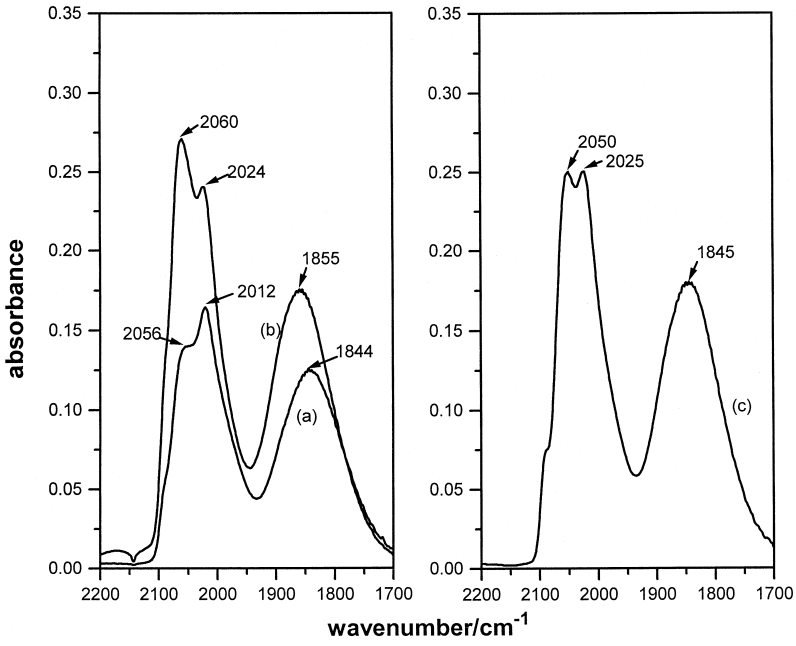

Fig. 2. Spectra of $Rh(B)/SiO_2$ after methane treatment (673 K) and addition of CO (293 K) at (a) < 1 and (b) 3.6 kN m^{-2}, and (c) subsequent evacuation (293 K, 20 min).

CO coverages (Fig. 2b). The shift could also be attributed to a decrease in dipole coupling between adjacent CO molecules combined with increased electron donation from rhodium to CO. However, the deposition of carbon may have also induced a different bridging mode of adsorption of CO. Thus, for example, $Rh_2(CO)_3$ may give a band at ca. 1900 cm^{-1}, close to the present band at 1898 cm^{-1} for untreated catalyst, whereas Rh_2CO gives a band at 1845–1875 cm^{-1} [19]. Changes involving gem-dicarbonyl species were more difficult to recognize because of overlap with the band due to linear CO. A band at 2012 cm^{-1} shifting to 2024 cm^{-1} at high coverage was more prominent than the band at 2031 cm^{-1} for the untreated surface, although the intensity of the band maximum was less than that for the untreated Rh/SiO_2, possibly in part because of the great reduction in the overlapping linear CO band. The other gem-dicarbonyl band had moved from 2097 cm^{-1} (Fig. 1) to become a shoulder at ca. 2085 cm^{-1} (Fig. 2), again with a slight loss in apparent intensity. In general, therefore, the inhibition of CO adsorption was in the order linear CO > bridged CO > gem-dicarbonyl, with band shifts to lower wave numbers for all three species. There was no evidence for the shoulder at 1965 cm^{-1} (Fig. 1) in the spectra of methane-treated Rh/SiO_2, suggesting the absence of $Rh_2(CO)_3$ species. CO adsorbed on the methane-treated surface was resistant to desorption at room temperature, although the band due to linear CO was slightly weakened, and the band due to bridged CO shifted to 1845 cm^{-1} albeit with no change of intensity.

Spectra of CO on $Rh(A)/SiO_2$ (Fig. 3) gave a greater intensity per percentage Rh of the band due to linear CO, than on $Rh(B)/SiO_2$. In addition, the bridged/linear intensity ratio was smaller for Rh(A) than for Rh(B). However, in the bridging region, there was clearer evidence (Fig. 3a) for two bands at 1893 and 1860 cm^{-1}, showing the availability of two types of adsorption site for Rh_2CO species. The formation of gem-dicarbonyl was less prevalent for Rh(A) than for Rh(B). Broadly speaking, the effects of heat treatment in methane were similar for the

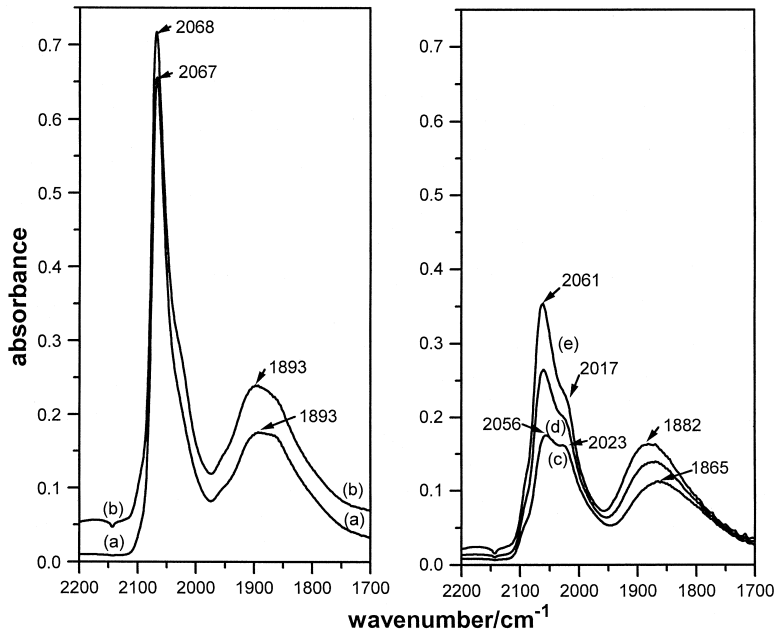

Fig. 3. Spectra of Rh (A)/SiO_2 after the addition of CO at (a) <1 and (b) 3.6 kN m^{-2}. Spectra of Rh(A)/SiO_2 after methane treatment (673 K) and subsequent addition of CO (293 K) at (c) <1, (d) 1.2 and (e) 3.6 kN m^{-2}.

two catalysts, although CO was less impeded by coking on Rh(A) than on Rh(B) (Fig. 3). For Rh(A), the intensity of the linear CO band was reduced by 48% and the bridged band was only reduced by 14%. Furthermore, the bridged band only shifted to 1882 cm^{-1} at high coverage on Rh(A), compared with the shift to 1855 cm^{-1} for Rh(B).

Coked Rh(A)/SiO_2 was subjected to further treatment in hydrogen at three temperatures before CO adsorption, in order to probe the reactivity of coke deposits towards hydrogen. Treatment at 293 K failed to regenerate CO adsorption sites (Fig. 4A). All the band intensities were less than for CO on coked Rh(A). This may have arisen because of hydrogen adsorption, which under the influence of coke, impeded subsequent adsorption of CO, or because surface coke was partially hydrogenated to give a new surface species which impinged on more surface Rh atoms. The presence of coke weakened the adsorption of CO on Rh/SiO_2 (Figs. 1 and 2), thus, decreasing the possibility of H-adatoms being displaced from the surface by CO. Residual sites were influenced by coke or hydrogen adatoms. Bands at 2061, 2017 and 1865 shifting to 1882 cm^{-1} (Fig. 3) for coked Rh(A) appeared at 2056, 2021 and 1848 shifting to 1861 cm^{-1} (Fig. 4A) for hydrogen-treated coked Rh(A). The latter results resembled the band behaviour for Rh(B) after coking (Fig. 2).

Hydrogen treatment of coked Rh(A) at 373 K gave results for linear and bridged CO similar to those following hydrogen treatment at 293 K (Fig. 4B). However, bands at 2090 and 2025 cm^{-1} due to rhodium dicarbonyl were much more prominent, suggesting the occurrence of disruption of rhodium crystallites leading to Rh^I species. By analogy, CO produces a disruptive effect on rhodium, which leads to an enhancement of adsorbed gem-dicarbonyl, although the effect in that case is suppressed by hydrogen above 373 K [20,21]. The gem-dicarbonyl was less prominent after hydrogen treatment at 473 K (Fig. 4C). The level of adsorption of linear CO was above that after hydrogen treatment at 293 or 373 K and was closely similar to that for coked Rh(A). Thus, hydrogen had been desorbed during evacuation at 473 K, releasing sites for CO adsorption. However, hydrogen at

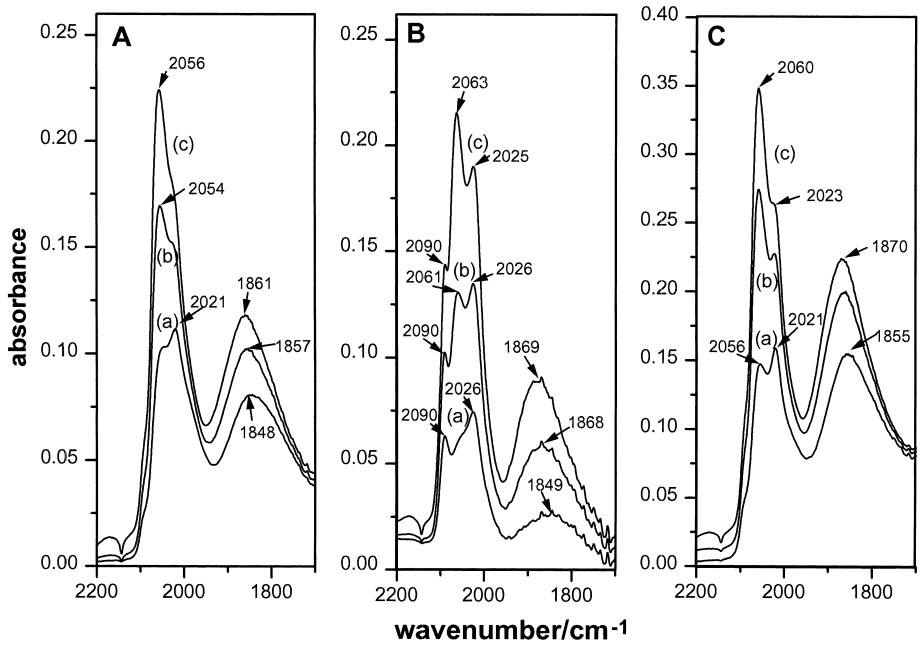

Fig. 4. Spectra of Rh(A)/SiO_2 after methane treatment (673 K) and hydrogen treatment at (A) 293 K, (B) 373 K and (C) 473 K before admission of CO at (a) < 1, (b) 1.2 and (c) 3.6 kN m^{-2}.

473 K had failed to free any of the linear sites which had become coked during treatment in methane. In contrast, the band due to bridged CO had recovered to its intensity, or was even of slightly greater intensity, than the corresponding band for uncoked Rh(A). However, the band was at 1870 cm^{-1} for high CO coverage, still somewhat lower than the 1882 cm^{-1} for Rh(A) before hydrogen treatment. Bridged sites were not poisoned, but remained influenced by retention of hydrocarbonaceous residue on the rhodium surface. The shoulder at ca. 1965 cm^{-1} for uncoked Rh was not regenerated by hydrogen treatment after coking. The formation of $Rh_2(CO)_3$ remained poisoned, although the slight enhancement in the band at 1870 cm^{-1} may have been because the sites had become more favourable for Rh_2CO formation.

3.2. CO adsorption on Cu–Rh / SiO_2

Spectra of CO on Cu–Rh(C)/SiO_2 (Fig. 5) contained a strong band at 2061 cm^{-1} due to linearly adsorbed CO on Rh, but no evidence for bands due to gem-dicarbonyl. In accordance with this result, the hydrogen adsorption data (Table 2) showed that of all the catalysts studied, Cu–Rh(C) gave the lowest H/Rh ratio. The band shift from 2071 cm^{-1} for Rh(B)/SiO_2 shows an influence of the copper component on the exposed rhodium sites. Greater effects were apparent in the bridging spectral region. A band at 1864 cm^{-1} (Fig. 5) corresponded to a shoulder for rhodium alone (Figs. 1 and 3). However, the stronger band at ca. 1895 cm^{-1} for the latter was absent for Cu–Rh, showing that at least one type of bridging Rh–Rh site was destroyed by the presence of copper. In contrast, a shoulder at 1972 cm^{-1}, probably also due to a bridging CO complex [19], was much more intense for Cu–Rh than any possible band in a similar position for Rh alone.

Bands due to linearly adsorbed CO on copper sites in Cu–Rh(C)/SiO_2 were at 2133 and 2190 (vw) cm^{-1} (Fig. 5). A band at 2190 cm^{-1} has been reported for CO at Cu^{2+} sites in CuY zeolites [22]. The band at 2133 cm^{-1} may also be ascribed to CO ligated to cationic copper

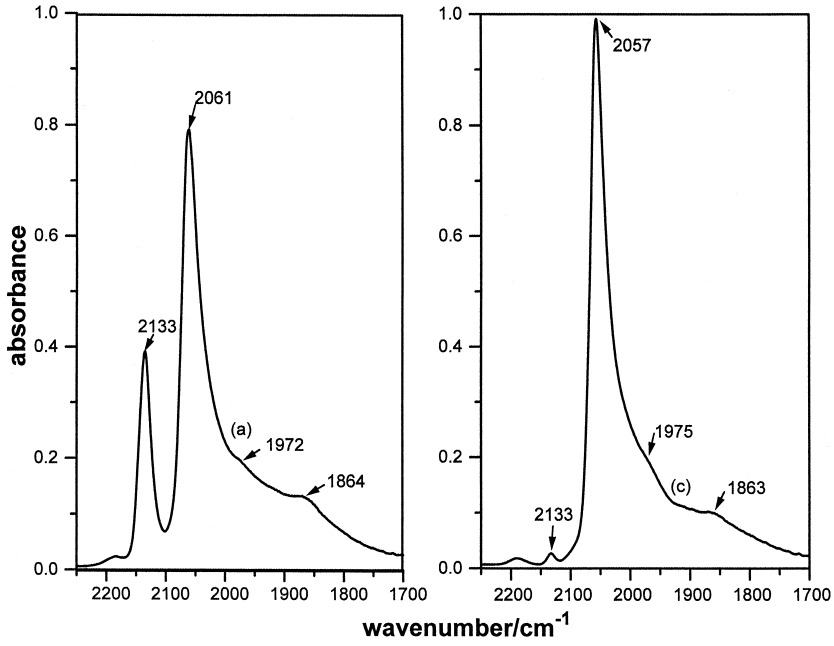

Fig. 5. Spectra of Cu–Rh(C)/SiO_2 (a) in the presence of CO (3.6 kN m^{-2}) and (b) after subsequent evacuation (293 K, 20 min).

[22–25]. Mendes and Schmal [11] assigned a band at 2134 cm^{-1} for Cu–Rh/Al_2O_3 to CO ligated to Cu^+ sites, and a similar band was also reported by Guerrero-Ruiz et al. [26].

Evacuation of Cu–Rh(C) at 293 K after adsorption of CO led to a slight decrease in band intensity at 1864 cm^{-1}, little change at 1972 cm^{-1} and an 18% increase in absorbance at the band maximum at 2061 cm^{-1} which shifted to 2057 cm^{-1} (Fig. 5a). This apparent increase in intensity was, however, accompanied by band narrowing, such that the integrated band intensity remained about the same. In contrast to the retention of CO on rhodium, the CO on copper giving the band at 2133 cm^{-1} was readily desorbed. The weak band at 2190 cm^{-1} was unaffected by evacuation (Fig. 5b).

Reaction of Cu–Rh(C)/SiO_2 with methane partially poisoned both Cu and Rh sites for CO adsorption (Fig. 6). The band due to CO on Cu was 28% of its intensity in the absence of coking, and was shifted to 2128 cm^{-1}. The band due to linear CO on Rh was 30% of its intensity without coking, and was shifted to 2051 cm^{-1}. The band at 2021–2025 cm^{-1} for rhodium alone (Figs. 2 and 3) was not apparent in the spectra of Cu–Rh, although broadening of the linear CO band towards lower wave numbers hinted at its presence which was probably obscured by the shift of the Rh–CO from

Table 2
Uptakes for hydrogen adsorption before and after coking

Catalyst	wt.% Rh	Hydrogen adsorbed/μmol g^{-1}		Apparent H/Rh ratio	
		Uncoked	Coked	Uncoked	Coked
Cu–Rh(A)/SiO_2	3.40	70.1	60.9	0.42	0.37
Cu–Rh(B)/SiO_2	5.04	87.8	77.9	0.36	0.32
Cu–Rh(C)/SiO_2	6.63	83.2	66.9	0.26	0.21
Rh(B)/SiO_2	5.00	85.5	73.6	0.35	0.30

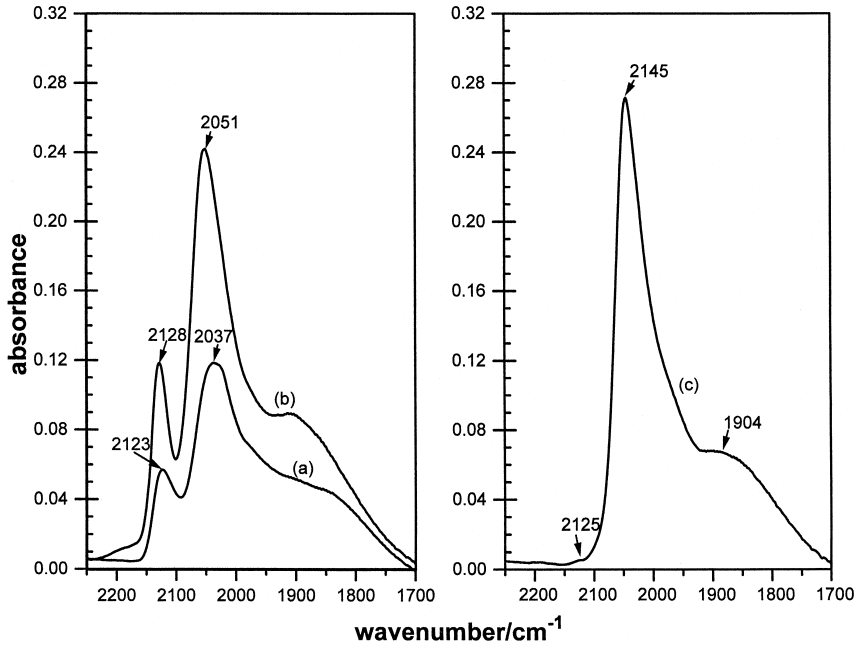

Fig. 6. Spectra of Cu–Rh(C)/SiO_2 after methane treatment (673 K) and admission of CO at (a) <1 and (b) 3.6 kN m^{-2}, and (c) subsequent evacuation (293 K, 20 min).

2061 cm^{-1} for Rh to 2051 cm^{-1}. In the bridging CO region, the band at 1864 cm^{-1} was apparent at low coverages (Fig. 6a), but never attained the intensity recorded for uncoked Cu–Rh. The shoulder at 1972 cm^{-1} was also much weaker for coked rather than for uncoked Cu–Rh. The dominant band in the bridging region for coked Cu–Rh was at 1904 cm^{-1}. This band was not identified for uncoked catalyst; nevertheless, it could have been present, but was obscured by the overlap with the two broad bands on either side (Fig. 5). The overall absorbance at 1904 cm^{-1} was less for coked than for uncoked catalyst, despite the enhanced prominence of the band at 1905 cm^{-1} for the former. In general, bridged CO sites on Rh in Cu–Rh were impeded less by coking than linear CO sites on either Rh or Cu. The effects of evacuation of coked Cu–Rh after exposure to CO (Fig. 6c) were similar to the results for uncoked Cu–Rh.

Subsequent treatment of coked Cu–Rh(C)/SiO_2 in hydrogen at 473 K had no effect on the intensity of the band at 2128 cm^{-1}, showing that copper sites had remained poisoned. The band at 2051 cm^{-1} was 15% more intense than for coked Cu–Rh, suggesting that some of the linear CO sites on Rh, which were poisoned by coking, had been regenerated. In the spectral region for bridging CO on Rh, the intensities of absorption at 1972 and 1904 cm^{-1} were similar for coked and hydrogen-treated coked Cu–Rh. However, hydrogen treatment did promote slight recovery of the band at 1863 cm^{-1}.

Cu–Rh(B)/SiO_2 contains the same percentage rhodium content as Rh(B)/SiO_2, therefore, comparison of results for the two catalysts provides a direct indication of the effects of 1% Cu on the surface character of Rh and its CO adsorption properties. The band due to linear CO on Rh was shifted -14 cm^{-1} to 2057 cm^{-1} for Cu–Rh(B), compared with -10 cm^{-1} for Cu–Rh(C). There are two possible causes of these shifts. First, electron transfer from Cu to Rh leads to electron-rich Rh sites, hence, in-

creasing back donation to $\pi*$ orbitals of adsorbed CO, thus, weakening the CO bond [27]. Second, dipolar coupling between CO molecules on adjacent sites is decreased by dilution of the Rh surface by Cu atoms, therefore, the CO band remains at a low position even at high coverage of the total surface [28]. Toolenaar et al. [28] and Hendrickx et al. [29] have shown that the latter effect is dominant for Pd–Cu and Pt–Cu catalysts, for which the electronic effect is very small. The bands at 1947 and 1854 cm^{-1} (Fig. 7) due to bridging CO species were similarly red-shifted from their positions for Cu–Rh(C) or Rh alone. There was no evidence for gem-dicarbonyl species. The shifts in the positions of all the bands due to CO on Rh on adding Cu to the catalyst show that all the exposed Rh atoms were influenced by the presence of Cu. The shifts are probably due to dipolar coupling effects [28,29], therefore, it is implied that Rh sites exist in surfaces which also contain Cu atoms. The intensities at the absorbance maxima of the dominant bands due to linear CO and bridge-bonded CO for Cu–Rh(B) were both 66% of the values for Rh(B), showing that the addition of Cu to 5% Rh had reduced the numbers of the types of Rh site responsible for these particular bands. However, the band at 1947 cm^{-1} (Fig. 7) was absent or at most much weaker for Rh (Fig. 1), suggesting that a new type of site had been created in the mixed metal catalyst. Hydrogen chemisorption gave nearly identical H/Rh values for Cu–Rh(B) and Rh(B) (Table 2). The results imply that there were the same number of exposed Rh atoms in the two catalysts, but the addition of Cu had caused a diminution of types of site present for Rh alone, but this was balanced by the appearance of a least one new type of bridging site. The band for CO on cationic copper sites was at 2132 cm^{-1} for Cu–Rh(B).

The main maxima due to linear and bridged CO on Cu–Rh(B) which had been heated in methane were reduced to 31% of their intensities for uncoked catalyst (Fig. 8). The Rh–CO band was at 2049 cm^{-1}, a band shift of -8 cm^{-1} caused by coking. As for Cu–Rh(C), a band at 1904 cm^{-1} became prominent for coked

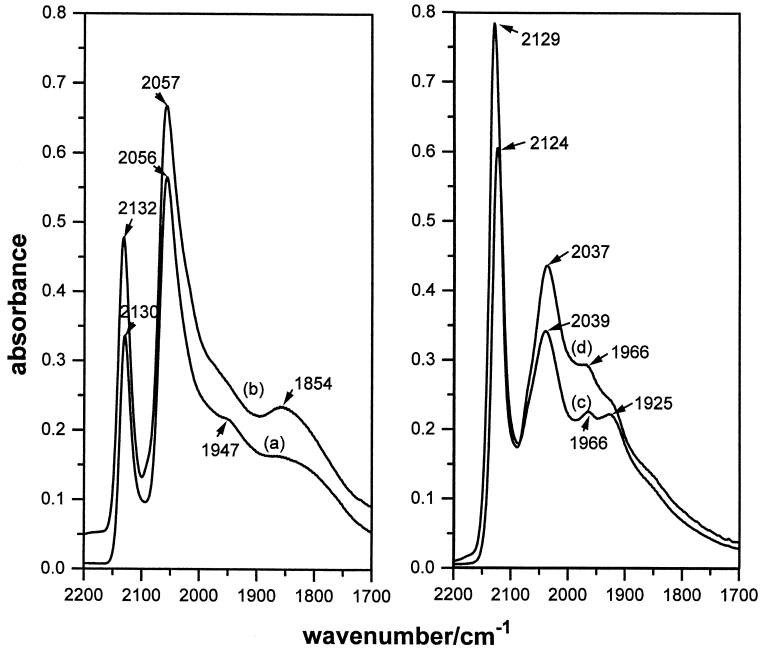

Fig. 7. Spectra of (a),(b) Cu–Rh(B)/SiO_2 and (c),(d) Cu–Rh(A)/SiO_2 exposed to CO at (a),(c) < 1 and (b),(d) 3.6 kN m^{-2}.

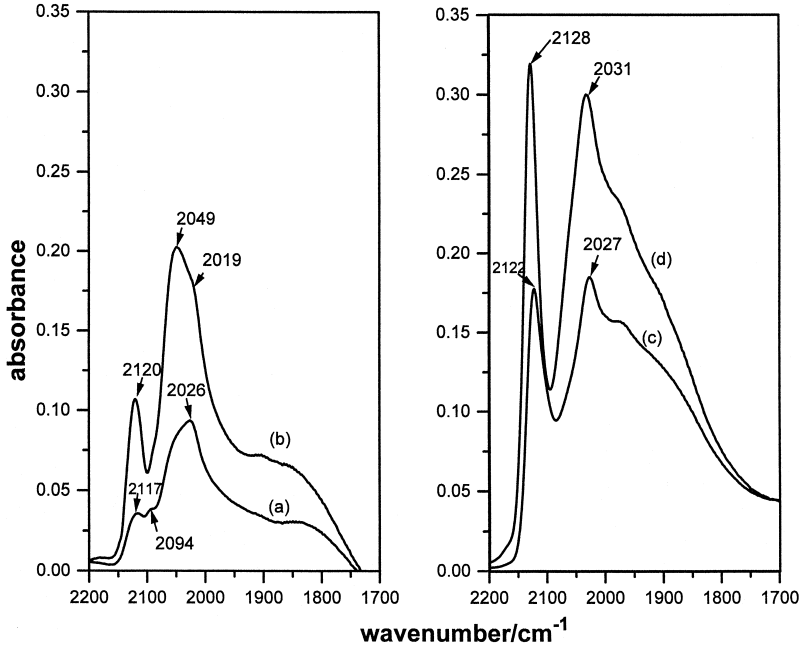

Fig. 8. Spectra of (a),(b) Cu–Rh(B)/SiO_2 and (c),(d) Cu–Rh(A)/SiO_2 after methane treatment (673 K) and admission of CO at (a),(c) < 1 and (b),(d) 3.6 kN m^{-2}.

Cu–Rh(B). Together with reductions in intensities caused by site poisoning, and band shifts due to dipolar coupling or electronic effects, the appearance of the band at 1904 cm^{-1} (Fig. 8) constituted a significant difference between the results for Rh(B)/SiO_2 (Fig. 2) and Cu–Rh(B)/SiO_2. Also, bands at 2094 and 2019 (sh) cm^{-1} due to surface gem-dicarbonyl were clearly visible. Poisoning of Cu was greater than that of Rh, the band at 2120 cm^{-1} being only 22% of its intensity for uncoked Cu–Rh(B). Evacuation at 293 K had similar effects on the CO spectra as for Cu–Rh(C).

Treatment of Cu–Rh(B) in hydrogen at 473 K after coking partially restored sites for the linear adsorption of CO on both Rh and Cu (Fig. 9). There was also a slight growth in absorbance in the bridging spectral region, although the band at 1904 cm^{-1} was less prominent. Gem-dicarbonyl species were not recognisable for the hydrogen-treated catalyst.

Fig. 10 contains the results for Cu–Rh(A)/SiO_2, as well as Figs. 7–9. The strong band due to CO on cationic Cu sites was at 2129 cm^{-1} (Fig. 7), continuing the trend that the lower the wave numbers, the higher was the Cu content of the catalyst. This was accompanied by a parallel downward trend in the position of the Rh–CO band with increasing Cu. The band position at high coverage was 2037 cm^{-1}. Similar trends have been discussed by Toolenaar et al. [28] for mixed metal systems, and have been ascribed to geometric, rather than electronic effects. An upward shift for Cu–CO on alloying with platinum was attributed to 'individualisation' of Cu atoms in the Pt surface [28]. In the bridging region, a weak shoulder at 1850 cm^{-1} was accompanied by maxima at 1966 and 1925 cm^{-1} (Fig. 7), the latter, in particular, not being discernable for any of the other catalysts.

Coking Cu–Rh(A)/SiO_2 reduced the Cu–CO band intensity by 59% with ca. -1 cm^{-1} shift to 2128 cm^{-1}, and the Rh–CO band intensity by 36% with a -6 cm^{-1} shift to 2031 cm^{-1} (Fig. 8). Band overlap in the bridging region led

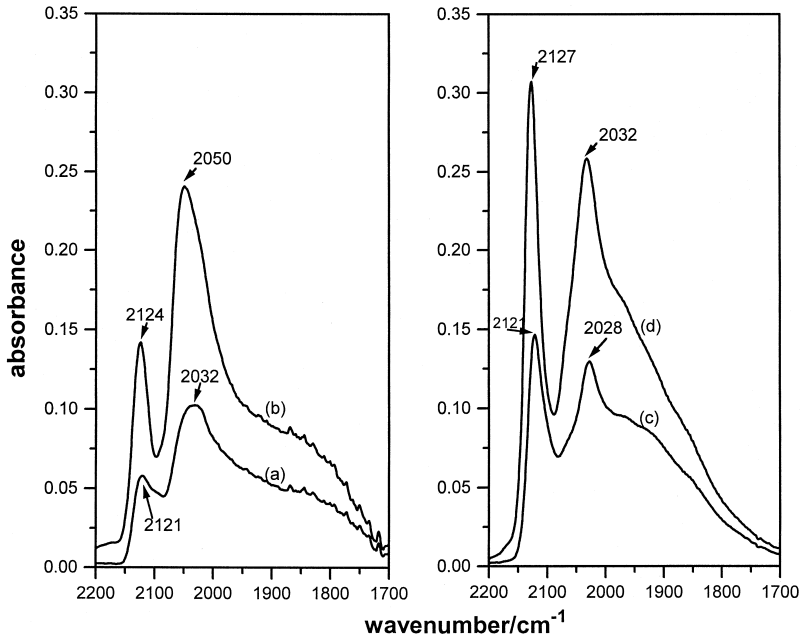

Fig. 9. Spectra of (a),(b) Cu–Rh(B)/SiO_2 and (c),(d) Cu–Rh(A)/SiO_2 after treatment in methane (673 K) and then hydrogen (473 K) before admission of CO (293 K) at (a),(c) < 1 and (b),(d) 3.6 kN m^{-2}.

to no clear maxima although shoulders existed at 1968 and 1899 cm^{-1}. The former was only 20% weaker than the corresponding band for uncoked Cu–Rh, suggesting that bridging sites were less susceptible to coking than linear sites on either Cu or Rh. Evacuation at 293 K for 20

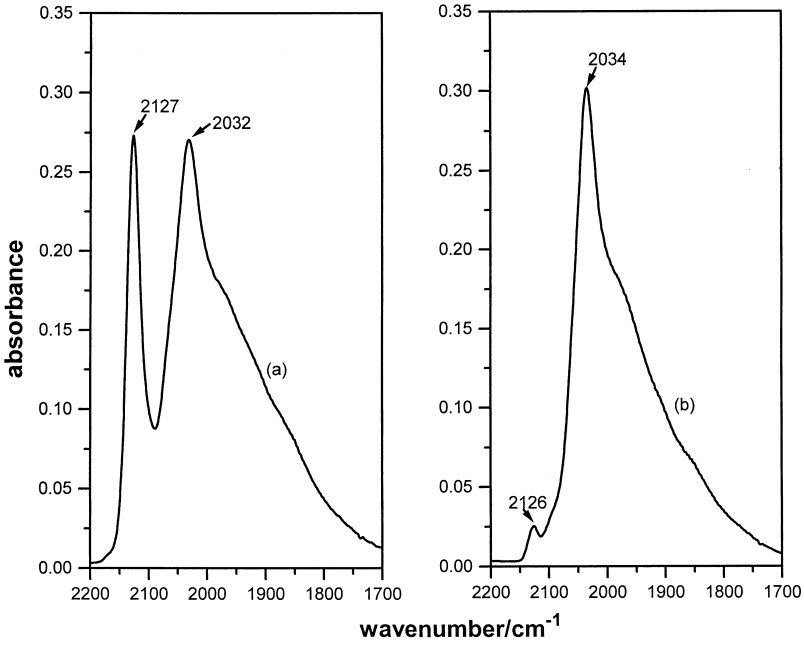

Fig. 10. As for Cu–Rh(A)/SiO_2 in Fig. 9, followed by evacuation (293 K) for (a) 30 s and (b) 20 min.

min removed 92% of the CO from Cu sites, but only $< 12\%$ of the CO on Rh. Heat treatment of coked Cu–Rh(A) in hydrogen before adsorption of CO gave spectra (Fig. 9) which were very similar to the results for coked catalyst (Fig. 8).

One general result for all the catalysts was that the attainment of maximum surface coverage by CO occurred at a much lower CO pressure for uncoked catalyst. This is illustrated by the spectra in Figs. 3–5. Spectra 3(a), 3(c), 4A(a) and 4B(a) all correspond to the same low pressure of CO, whereas spectra 3(b), 3(e), 4A(c) and 4B(c) are all for the same high pressure of CO. Fractional surface coverage of the available adsorption sites increased more steeply as a function of CO pressure for uncoked, rather than for coked catalysts. A possible explanation would be that CO adsorption was weaker on both Cu and Rh sites in coked catalyst. However, the effects of evacuation at 295 K showed that while CO could be readily desorbed from Cu sites, desorption from Rh did not occur. Coke residues are known to retain mobility at low temperatures and may undergo ordering into islands in the presence of CO [30]. The present adsorption and desorption behaviour would be explicable if ordering occurred, the degree of ordering was enhanced by increasing CO pressure and ordering enhanced the availability of Cu and Rh sites for CO adsorption.

3.3. CO adsorption on Cu/SiO_2

Results for Cu/SiO_2 were similar to those of Guerrero-Ruiz et al. [26] for Cu/Al_2O_3 in the sense that the temperature of reduction had an influence on the position and intensity of the infrared band due to subsequently adsorbed CO. Our previous results for Cu/SiO_2 calcined at 623 K and then reduced at 623 K gave a strong maximum at 2099 cm^{-1} [24]. For the present catalyst, the band was at 2104 cm^{-1}. However, calcination at 673 K followed by reduction at 673 K resulted after CO adsorption in a much weaker maximum at 2118 cm^{-1} (Fig. 11). Adsorption of CO on Cu/SiO_2 pre-treated with N_2O gives a similar band at 2118 cm^{-1} which was attributed to cationic Cu sites [24]. Heat treatment in methane before admission of CO had little effect on the result, in terms of either band intensity or position (Fig. 11b). CO adsorption sites on copper alone were not poisoned by the methane treatment. Solymosi and Cserényi [8] have also reported that methane did not decompose over Cu/SiO_2. The poisoning of copper sites in Cu–Rh catalysts must, therefore, have resulted from methane decomposition on Rh and spill-over onto exposed Cu. CO was readily desorbed from copper by evacuation at 293 K (Fig. 11).

3.4. Hydrogen chemisorption

Hydrogen uptakes by the catalysts obtained by extrapolation to zero pressure are given in Table 2. Apparent H/Rh ratios for uncoked catalysts are estimated on the assumption that all the hydrogen adsorption occurred at Rh sites. The nearly identical results for Cu–Rh(B) and Rh(B), which have similar Rh loadings, show that the addition of 1.11% Cu to 5% Rh had little effect on the total number of Rh sites, although the infrared results showed that there were changes in site character. The addition of Cu to Rh/Al_2O_3 has been shown to increase the hydrogen uptake at low copper loadings, but decreases the uptake at higher loadings [10,13]. For Rh (2.4 wt.%)/SiO_2 with added copper ($Cu/Rh = 0.33$), Coq et al. [31] reported that the surface composition was $Cu/Rh = 1.0$, implying that enrichment with copper had occurred in the exposed surfaces of the mixed metal catalyst. The previous data for Cu addition to Rh/SiO_2 at a fixed Rh loading [31] show that the present trends for Cu–Rh may be primarily attributed to the effects of Rh loading on dispersion, with a higher loading giving a lower H/Rh value. The variations in bulk mole fraction of copper here (0.15, 0.26 and 0.42 for Cu–Rh(C), (B) and (A), respectively) should

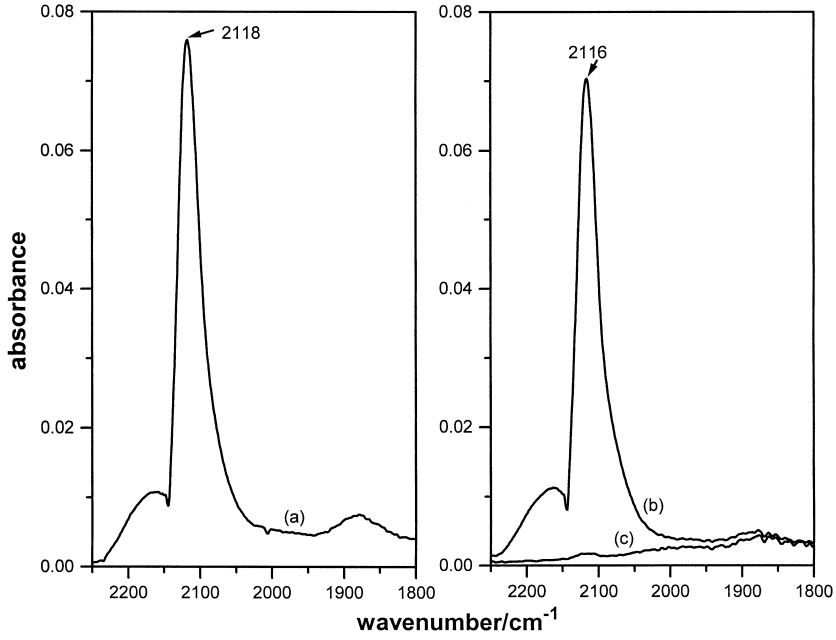

Fig. 11. Spectra of Cu/SiO_2 (a) exposed to CO (3.6 kN m^{-2}), (b) exposed to CO (3.6 kN m^{-2}) after treatment with methane (673 K), and (c) subsequent evacuation.

give ca. 25% decrease in dispersion with increasing Cu concentration. This opposes the observed trend towards better dispersion, which must therefore be dominated by effects due to the decreasing Rh loading as the Cu content was simultaneously increased.

The results for coked catalysts exhibited the same trends as those for uncoked samples, but the hydrogen uptakes were reduced by 12–19%. These reductions are much less than that expected from the effects of coking on the intensities of infrared bands due to adsorbed CO. Maxima due to Rh–CO were reduced by 36–70%. Bands due to bridging CO were less sensitive to coking, but still gave intensity reductions up to 38%. One explanation for the discrepancy would be that steric effects of surface carbonaceous residue impede CO adsorption, but do not impede the generation of hydrogen adatoms. In the present static volumetric measurements, it is also possible that the results were influenced by the reaction of hydrocarbonaceous material with hydrogen. The catalysis results showed that methane was generated from hydrogen and coked catalyst at temperatures as low as 323 K. Lower reaction temperatures have been reported [1,2]. If, for example, the following reaction occurred at 293 K,

$$Rh{-}CH_{3(ads)} + H_{2(g)} \rightarrow Rh{-}H_{(ads)} + CH_{4(g)},$$

this would not lead to a change in the gas-phase pressure. The similar reaction of surface residue with structure equivalent to $Rh{-}CH_2$ groups would give the same drop in gas pressure as for hydrogen on an uncoked surface. Thus, high surface poisoning for CO adsorption would not be replicated by estimates of hydrogen adsorption based on pressure measurement.

3.5. Reaction of coked catalyst with hydrogen

The dominant product of the reaction of hydrogen with coked catalysts was methane. Fig. 12A shows the methane evolution as a function of the temperature of the reaction for $Rh(A)/SiO_2$. Maximum methane formation occurred at 388 K. The two points included in Fig. 12A for 423 K were for different reaction times, and illustrate the fall-off in the rate of methane

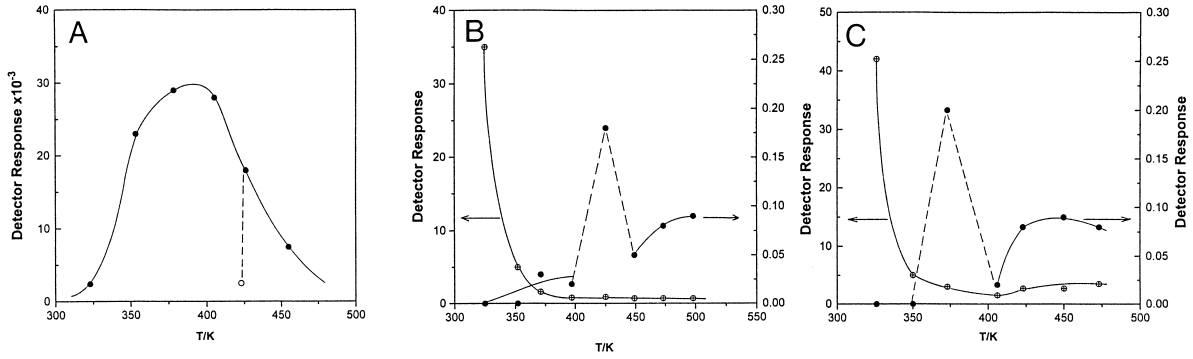

Fig. 12. (A) Methane evolution from coked Rh(A)/SiO_2, as a function of the temperature of the reaction with hydrogen after 5 min (O) and 20 min (O) at each temperature. (B) Methane (⊕) and ethane (O) formation from the reaction of coked Cu/SiO_2 with hydrogen. (C) Methane (⊕) and ethane (O) formation from the reaction of coked Cu–Rh(C)/SiO_2 with hydrogen.

formation with time at a given temperature. Ethane was also formed at a level of ca. 1% of the methane formed.

Results for Cu/SiO_2 (Fig. 12B) and Cu–Rh(C)/SiO_2 (Fig. 12C) showed a rapid tail-off in methane production to low levels above ca. 353 K. Ethane formation remained low, but showed maxima at 423 and 503 K for Cu and at 393 and 453 K for Cu–Rh(C). The occurrence of the higher-temperature maxima in reaction profiles for Rh–MoO_3/SiO_2 and Rh–MoO_3/SiO_2 catalysts is being currently investigated [32]. The results for Rh(B)/SiO_2 showed maxima at ca. 473 K for both methane and ethane formation.

4. Discussion

A summary of the positions of the main infrared bands reported here for uncoked and coked catalysts is given in Table 3. The band positions for coked catalysts after treatment in hydrogen were only altered slightly from the values for coked catalyst.

4.1. Uncoked catalysts

Copper and rhodium are partially miscible in the bulk [9]. For Cu–Rh/Al_2O_3, it has been proposed that the catalysts are composed of segregated phases of copper and rhodium and alloyed clusters [26]. In contrast, the present infrared bands, particularly for linear CO on rhodium in the presence of copper and on copper in the presence of rhodium, showed no evidence for linear rhodium or copper sites which were not influenced by the second metal. All exposed surfaces apparently contained both metal components. Furthermore, there was no evidence from the bands due to linearly adsorbed CO for two types of surface alloy, a Rh-rich phase and a Cu-rich phase, which have also been reported for Cu–Rh/Al_2O_3 [10]. The complexity of the spectra with several overlapping bands in the CO-bridging region precludes

Table 3
Band positions (ν/cm^{-1}) for linear and bridged CO on Cu and Rh sites

Catalyst	Cu–CO	Rh–CO	Bridging CO		
Uncoked					
Cu	2118				
Cu–Rh(A)	2129	2037	1966	1925	1850 (sh)
Cu–Rh(B)	2132	2057	1947 (sh)		1854
Cu–Rh(C)	2133	2061	1972 (sh)		1864
Rh(A)		2068	1950 (sh)	1893	1860 (sh)
Rh(B)		2071	1949 (sh)	1898	1860 (sh)
Coked					
Cu	2116				
Cu–Rh(A)	2128	2031	1968 (sh)	1899 (sh)	1865 (sh)
Cu–Rh(B)	2120	2049		1904	1855 (sh)
Cu–Rh(C)	2128	2051	1972 (sh)	1904	1864 (sh)
Rh(A)		2061		1882	
Rh(B)		2060			1855

any judgement of whether bridged sites might have existed on two surfaces of different alloy composition.

Despite a report of Rh-rich surfaces in Cu–Rh/Al_2O_3 [11], other studies of Cu–Rh/Al_2O_3 [10] and Cu–Rh/SiO_2 [9,31] suggest that copper enrichment occurs in the surface of mixed metal particles. Here, the intensities of the linear Cu–CO bands for Cu–Rh catalysts were greater than the corresponding intensity for Cu/SiO_2, suggesting that copper enrichment in the surface had occurred. However, this conclusion relies on the possibly dubious assumption that the extinction coefficient of the Cu–CO band was insensitive to the changing character of the Cu sites. Comparison of the ratio of intensities of the bands due to Rh–CO and Cu–CO with the stoichiometric Rh/Cu ratios shows that the ratio of RhCO to CuCO sites in the surface was proportional to the Rh/Cu composition for Cu–Rh(A) and Cu–Rh(C), but for Cu–Rh(B), there was enrichment relative to the other two catalysts in Rh–CO. Thus, in terms of sites which adsorb linear CO, the overall enrichment of Cu was similar for catalysts (A) and (C), but less marked for Cu–Rh(B).

The similar hydrogen uptakes by Rh(B) and Cu–Rh(B), which had similar rhodium loadings, was accompanied by a 66% lower intensity infrared band due to linear Rh–CO for the latter, showing that copper had decreased the proportion of rhodium sites which adsorbed CO linearly. This was accompanied by losses and gains of band intensity (Figs. 1 and 7) in the bridging CO region, with a slight overall gain. The implication, therefore, is that addition of the copper component favoured bridging Rh sites at the expense of linear Rh sites. This is the opposite of what happens in other systems, for example, Cu–Pd, where the addition of copper favours linear CO on palladium at the expense of bridged sites [33]. The proposal that rhodium in Cu–Rh/SiO_2 occupies high coordination sites on dense planes [31] is consistent with the present conclusion, although the generation of new bands due to bridging CO for the copper-containing catalyst shows that copper atoms must also exist in the dense planes, hence, influencing the adsorption behaviour of the rhodium. Ksibi and Ghorbel [13] concluded that Cu–Rh catalysts formed bimetallic clusters which exhibit different properties from those for rhodium alone. Simple segregation theory based on the broken bond model predicts that the higher melting point metal (Rh) in mixed metal systems should stay on surface sites with the highest coordination.

Bridging Rh_2CO species on rhodium generally give an infrared band within the range 1845–1875 cm^{-1}, whereas bands at 1900–1925 cm^{-1}, or as high as 1949 cm^{-1} [15], are ascribed to $Rh_2(CO)_3$ [18,19]. Copper addition had little effect other than to induce a small intensity loss on the band present for rhodium alone as a shoulder at ca. 1860 cm^{-1}. Bridging sites giving this band were relatively unaffected by copper. However, sites giving the band at 1898 cm^{-1} (Fig. 1) were destroyed by copper. Band growth occurred in the range 1920–1990 cm^{-1} and, in particular, at 1925, 1966 and 1972 cm^{-1}. The band shifts were not due to dipolar coupling effects associated with dilution of the rhodium surface with copper atoms, but to the removal of one type of site and the creation of different sites. Bands at 1966 and 1972 cm^{-1} are unusual for CO on rhodium surfaces, although bands at 1967–1975 and 1972–1982 cm^{-1} have been recorded for dicarbonyl and monocarbonyl molecular complexes, respectively, of Rh^+ [36,37]. The former also give a band at 2043–2060 cm^{-1}. The ionisation potential of Rh is slightly less than that for Cu suggesting that if any charge transfer occurred between the two metals, it would generate $Rh^{\delta+}$ atoms. However, the attribution of the present bands to cationic sites appears unlikely, as copper inhibits the oxidation of rhodium atoms at least in Cu–Rh/Al_2O_3 catalysts [11].

Infrared studies of Cu–Rh/Al_2O_3 [26,31] gave a band at ca. 2135 cm^{-1}, which was ascribed to adsorption at Cu^+ sites, although the suggestion that these were in an aluminate phase

[26] is not tenable here for silica-supported catalyst. The present bands for CO on copper sites in Cu–Rh are in the spectral range which is normally held to typify adsorption on cationic Cu sites [11,22–26]. However, Toolenaar et al. [28] and Hendrickx et al. [29] have demonstrated that band shifts for linearly adsorbed CO on the metal components of mixed metal catalysts may predominantly be ascribed to dipolar coupling effects. The upward shift in the frequency of the Cu–CO band observed here for Cu–Rh on increasing the rhodium content of the catalyst resembles the same effect for increasing platinum in Cu–Pt on either alumina or silica [28]. The latter was attributed to 'individualisation' of copper atoms in the platinum surface. The downward shift in the linear Rh–CO band with increasing copper content of the catalysts is attributed to a decrease in dipolar coupling between adjacent CO molecules caused by dilution of the surface concentration of linear Rh sites by copper atoms in the surface [28,29].

Comparison of Figs. 1 and 7 for catalysts with the same rhodium content show, in accordance with the results for $Cu–Rh/Al_2O_3$ [34,35], that the addition of copper inhibited the formation of rhodium gem-dicarbonyl species, responsible here for bands at 2097 and 2033 cm^{-1}. Platinum has a similar effect in Pt–Rh catalysts [14]. These bands are associated with highly dispersed or isolated rhodium sites [18,19]. Dumas et al. [34] concluded that copper was deposited on exposed rhodium atoms with a low coordination number. Coq et al. [31] deduced that copper preferentially occupies low coordination sites, edges and corners in $Cu–Rh/SiO_2$. The blocking of low coordinated Rh atoms by Cu appears to decrease the propensity of Rh to undergo disruption in the presence of CO.

4.2. Effects of coking

In accordance with the present results, Solymosi and Cserényi [8] found out that methane did not react with Cu/SiO_2 at 473–773 K, and suggested that the CH_3 formed in the dissociation of methane on rhodium may migrate onto copper in $Cu–Rh/SiO_2$. The latter point is clearly proved here. For all three Cu–Rh catalysts, the linear adsorption of CO on copper was poisoned more than any of the adsorption sites on rhodium by heat treatment in methane. Besides site poisoning, an additional contributing factor could be gas-induced enrichment of Rh in exposed surfaces. The latter effect has been reported for Pt–Cu catalysts [38]. In general, intensity losses of IR bands incurred by methane treatment were in the sequence Cu–CO > Rh–CO > Rh_2CO (or $Rh_2(CO)_3$). The deposition of carbon by high-temperature CO treatment of Rh/Al_2O_3 inhibited the adsorption of CO to give gem-dicarbonyl species [18] in contrast to these data, where gem-dicarbonyl sites were retained after methane treatment of both Rh/SiO_2 (Fig. 4B) and $Cu–Rh/SiO_2$ (Fig. 8). Apart from the gem-dicarbonyl species for which the bands were too weak for quantitative comparison, all other types of surface site on both the copper and rhodium components of Cu–Rh were heavily poisoned by the decomposition products of methane at 473 K.

Spectra of CO on Rh/SiO_2 were similar to the results of Fisher and Bell [15]. Deposition of carbon on Rh/Al_2O_3 by CO treatment at 573 K led to a dominant infrared band at 2063 cm^{-1} after subsequent CO adsorption [18], resembling the present band at 2060 cm^{-1} for Rh/SiO_2 after methane treatment. The band due to linear CO on rhodium was shifted to lower wave numbers after methane treatment for Rh/SiO_2 and all three $Cu–Rh/SiO_2$ catalysts (Table 3). An explanation of the shift for Rh/Al_2O_3 invoked dipole coupling effects combined with electron transfer from carbon to rhodium which increases back donation to the $\pi*$ orbital of adsorbed CO, hence, weakening the CO bond. The latter explanation is inconsistent with the results for silica-supported catalysts, for which comparisons of the effects of added copper and carbon on the band positions and intensities are instructive.

Fig. 13 shows the correlation between Rh–CO band intensities and positions for uncoked catalysts, which illustrate the effect of copper on linearly adsorbed CO on Rh, and for coked catalysts which show the effects of the decomposition products of methane. For a particular loss of intensity, the shift (from 2071 cm^{-1} for uncoked Rh/SiO_2) due to copper, which may be primarily attributed to dipolar coupling effects [28,29], was much greater than the shift induced by methane treatment. One explanation might be that while copper is evenly distributed over or in the rhodium surface, the decomposition products aggregate in patches leaving areas of unmodified or only partially modified rhodium. Patches of coke inhibit CO adsorption, but residual rhodium areas behave, in terms of dipolar coupling effects, as if the surface coverage of Rh sites is much less than the total coverage of the rhodium surface. The band shift for a high total coverage would, therefore, be smaller than expected for an even distribution of products over rhodium. The aggregation of coke deposit into patches may be promoted by CO adsorption [30]. This constitutes an explanation of the results based on a geometric effect involving poisoning of adsorption sites by coke. However, a plausible alternative explanation invokes an electronic effect of coke, on Rh sites, hence, affecting CO adsorption.

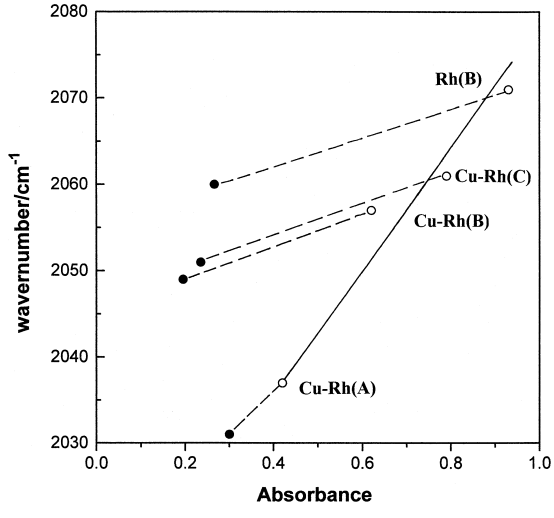

Fig. 13. Correlation between Rh–CO band positions and intensities for uncoked (O), and coked (O) catalysts.

If dipolar coupling effects of copper and coke deposits by dilution of the overlayer on Rh–CO are assumed to be similar, then, the results for coked catalysts suggest that two competing effects were responsible for the comparatively small Rh–CO band shifts induced by coking. For the inhibition of CO adsorption on ca. 70–80% of the linear Rh sites (Fig. 13), extrapolation of the data for the effects of copper in uncoked catalysts suggests that the band for Rh–CO on coked catalysts should be below 2030 cm^{-1}. The results for Rh/SiO_2 and Cu–Rh(B) and Cu–Rh(C), in particular, were well-above this, indicating that a further contributing factor was opposing the dipolar effect and shifting the band towards higher wave numbers. The probable formation of hydrocarbonaceous CH_x species on methane decomposition [4] will lead to the extraction of electrons from metal clusters [39–41]. Carbidic carbon [2] may do the same. Adsorption of CO at adjacent metal sites will, therefore, involve less electron donation to the antibonding CO orbitals, resulting in a stronger C–O bond, hence, resulting to an upward shift in the CO band position.

The geometric explanation of the infrared results is preferred over the electronic explanation. The latter probably contributes to the results, but cannot account for the contrast between the parallel growth of bands due to CO on Cu and Rh sites, and the considerably easier desorption of CO from Cu, rather than from Rh sites. The strengths of adsorption of CO on the Cu and Rh sites widely differ. The parallel growth of bands is attributed to the reorganisation of coke deposits promoted by CO.

The desorption characteristics of CO on Cu–Rh/SiO_2 showed that CO was much more weakly adsorbed on Cu sites than Rh sites. Despite the reported [8] inability of copper alone to decompose methane, coking of the copper component of Cu–Rh/SiO_2 catalysts occurred and led to intensity losses and red-shifts of the Cu–CO infrared band. This contrasted with the

effect of increasing rhodium content in the catalysts, for which loss of Cu–CO band intensity was accompanied by a blue-shift in the band position. The Cu–CO and Rh–CO band shifts incurred by methane treatment were closely similar, particularly for Cu–Rh(B) and Cu–Rh(C), therefore, it is tempting to ascribe the shifts for Cu–CO to the same effects as for Rh–CO. Thus, dilution of the surface concentration of Cu sites by coking leads to intensity losses for the Cu–CO band and a red-shift due to a decrease in dipolar coupling which is partially compensated by an electronic effect of decomposition products on copper sites which leads to weaker adsorption, but a stronger C–O bond.

4.3. Reaction of coked catalysts with hydrogen

Despite the absence of the inhibition of CO adsorption at Cu sites in Cu/SiO_2 catalysts and a report that methane does not react with Cu/SiO_2 at 473–773 K [8], the present Cu/SiO_2 catalyst treated with methane at 673 K did generate a very small amount of methane on subsequent reaction with hydrogen. The maximum amount was at the lowest temperature studied (325 K), therefore, it may be ascribed to a carbidic or C_α type of carbon [2,4,8]. The Cu–Rh catalysts behaved in the same way, in contrast to the results for Rh/SiO_2 which was many orders of magnitude more active for the formation of methane on hydrogenation. Copper has previously been shown to reduce or inhibit the activity of Rh in $Cu–Rh/SiO_2$ catalysts for methane decomposition, production of hydrocarbons from deposited carbon [8], or for the hydrogenation of benzene [13]. Solymosi and Cserényi [8] recorded a second maximum at > 500 K in the reactivity of hydrogen with carbon generated on Rh/SiO_2 by the reaction with methane at 573 K, and commented that the temperature for maximum activity was increased by increasing the temperature at which the deposited carbon was generated from methane. Here, the higher decomposition temperature (673 K) led to maximum hydrogenation activity at 388 K. This is, nevertheless, consistent with the hydrogenation of C_β type carbon which favours methane formation [2]. It appears that the reactivity of carbonaceous deposits on supported Rh towards hydrogen is extremely sensitive to the pre-treatment conditions during methane decomposition, therefore, detailed comparisons of results in the literature would be unwise [7]. In this context, the disappointing yields of ethane and absence of other products for the present catalysts contrast with the better yields obtained under different experimental conditions [8]. One argument for low yields of higher hydrocarbon is that simultaneous hydrogenolysis reactions within the catalyst bed are favoured [7].

Although infrared band positions for linear Cu–CO and Rh–CO for coked catalysts were fairly insensitive to hydrogenation, there were slight shifts induced by hydrogenation over Cu–Rh towards the positions for uncoked catalysts. This was accompanied by slight recovery of linear Cu and Rh sites showing that carbon associated with these sites was being hydrogenated. There was less evidence for recovery of sites on which CO could be adsorbed in a bridging configuration. In contrast, hydrogenation of coked Rh/SiO_2 gave no evidence for the recovery of linear sites from either band position or band intensity changes, but did, however, show evidence for recovery of bridged sites. Thus, although from the infrared results for CO adsorption, a higher proportion of linear sites on Rh/SiO_2 became poisoned by coking than bridging sites, it was the carbonaceous species at the latter which were more reactive towards subsequent hydrogenation. The addition of copper to Rh/SiO_2 significantly changed the character of bridging Rh sites, enhanced the level of poisoning of these Rh sites by coking and largely destroyed the activity of the catalysts for coke hydrogenation. In contrast, copper promotes low activity for the hydrogenation of coke at linear Rh sites. A previous report [8] showed that the effect of copper on the hydro-

genation reaction of coke deposits on Rh/SiO_2 was much less inhibiting than the result here, possibly because of a big difference between the coking conditions in the two studies.

Gem-dicarbonyl $Rh(CO)_2$ was a minority species on the Cu–Rh catalysts after CO adsorption, but was marginally more significant for Rh alone. The most prominent gem-dicarbonyl bands relative to Rh–CO, $Rh_2(CO)_3$ and Rh_2CO bands were for coked Rh/SiO_2 which was treated in hydrogen at 373 K (Fig. 4B). Low coordination sites favouring gem-dicarbonyl formation were promoted, suggesting that the disruption of Rh–Rh bonds generating isolated Rh^I sites [18,20] had occurred. The concentration of these sites was diminished by raising the hydrogenation temperature to 473 K. It is unlikely that gem-dicarbonyl Rh sites are important in the generation of higher hydrocarbons from coke hydrogenation [2,4].

References

[1] T. Koerts, R.A. van Santen, J. Chem. Soc., Chem. Commun. (1991) 1281.
[2] T. Koerts, M.J.A.G. Deelen, R.A. van Santen, J. Catal. 138 (1992) 101.
[3] M.M. Koranne, D.W. Goodman, Catal. Lett. 30 (1995) 219.
[4] G.C. Bond, Appl. Catal. A 149 (1997) 3.
[5] F. Solymosi, A. Erdöhelyi, J. Cserényi, Catal. Lett. 16 (1992) 399.
[6] A. Erdöhelyi, J. Cserényi, F. Solymosi, J. Catal. 141 (1993) 287.
[7] P. Ferreira-Aparicio, I. Rodriguez-Ramos, A. Guerrero-Ruiz, Appl. Catal. A 148 (1997) 343.
[8] F. Solymosi, J. Cserényi, Catal. Lett. 34 (1995) 343.
[9] G. Meitzner, G.H. Via, F.W. Lytle, J.H. Sinfelt, J. Chem. Phys. 78 (1983) 882.
[10] S.-C. Chou, C.-T. Yeh, T.-H. Chang, J. Phys. Chem. B 101 (1997) 5828.
[11] F.M.T. Mendes, M. Schmal, Appl. Catal. A 151 (1997) 393.
[12] V. Ponec, G.C. Bond, Stud. Surf. Sci. Catal. 95 (1995) 393.
[13] Z. Ksibi, A. Ghorbel, J. Chim. Phys. 92 (1995) 1418.
[14] J.A. Anderson, F. Solymosi, J. Chem. Soc., Faraday Trans. 87 (1991) 3435.
[15] I.A. Fisher, A.T. Bell, J. Catal. 162 (1996) 54.
[16] L.-W.H. Leung, D.W. Goodman, Catal. Lett. 5 (1990) 353.
[17] J.A. Anderson, C.H. Rochester, J. Chem Soc., Faraday Trans. 87 (1991) 1479.
[18] F. Solymosi, M. Lancz, J. Chem. Soc, Faraday Trans. 82 (1986) 883.
[19] C.A. Rice, S.D. Worley, C.W. Curtis, J.A. Guin, A.R. Tarrer, J. Chem. Phys. 74 (1981) 6487.
[20] F. Solymosi, F. Pásztor, J. Phys. Chem. 89 (1985) 4789.
[21] F. Solymosi, F. Pásztor, J. Phys. Chem. 90 (1986) 5312.
[22] A.A. Davydov, in: C.H. Rochester (Ed.), Infrared Spectroscopy of Adsorbed Species on the Surface of Transition Metal Oxides, Chap. 2, Wiley, Chichester, 1990.
[23] M.B. Padley, C.H. Rochester, G.J. Hutchings, F. King, J. Chem. Soc., Faraday Trans. 90 (1994) 203.
[24] G.J. Millar, C.H. Rochester, K.C. Waugh, J. Chem. Soc., Faraday Trans. 87 (1991) 1467.
[25] J. Szanyi, M.T. Paffett, Catal. Lett. 43 (1997) 37.
[26] A. Guerrero-Ruiz, B. Bachiller-Baeza, P. Ferreira-Aparicio, I. Rodríguez-Ramos, J. Catal. 171 (1997) 374.
[27] R. Liu, B. Tesche, H. Knözinger, J. Catal. 129 (1991) 402.
[28] F.J.C.M. Toolenaar, F. Stoop, V. Ponec, J. Catal. 82 (1983) 1.
[29] H.A.C.M. Hendrickx, V. Ponec, Surf. Sci. 192 (1987) 234.
[30] M. Salmeron, J. Dunphy, Faraday Discuss. 105 (1996) 151.
[31] B. Coq, R. Dutartre, F. Figueras, A. Rouco, J. Phys. Chem. 93 (1989) 4905.
[32] J.A. Anderson, C.H. Rochester, Z. Wang, unpublished results.
[33] S.S. Ashour, J.E. Bailie, C.H. Rochester, J. Thomson, G.J. Hutchings, J. Mol. Catal. A, Chem. 123 (1997) 65.
[34] J.M. Dumas, C. Géron, H. Hadrane, P. Marécot, J. Barbier, J. Mol. Catal. 77 (1992) 87.
[35] J. Barbier, J.M. Dumas, C. Géron, H. Hadrane, Appl. Catal. 67 (1990) L1.
[36] L.M. Vallarino, Inorg. Chem. 4 (1965) 161.
[37] F. Faraone, C. Ferrara, E. Rotondo, J. Organomet. Chem. 33 (1971) 221.
[38] A.D. Vanlangeveld, F.C.M.J. Vandelft, V. Ponec, Surf. Sci. 134 (1983) 665.
[39] F.J. Feibelman, Phys. Rev. B 26 (1982) 5347.
[40] T. Koerts, R.A. van Santen, J. Mol. Catal. 70 (1991) 119.
[41] J.A. Anderson, M. Fernández-García, G.L. Haller, J. Catal. 164 (1996) 477.